J | P | S | T

http://jpst.irost.ir

Journal of Particle Science and Technology

IROST

Investigation of mass transfer coefficients in irregular packed liquid-liquid extraction columns in the presence of various nanoparticles

Ali Vesal, Ahmad Rahbar-Kelishami*, Toraj Mohammadi

[1] *Department of Chemical Engineering, Iran University of Science and Technology (IUST), Tehran, Iran*

HIGHLIGHTS

- In this study, the effect of various nanoparticles on the mass transfer coefficient was investigated.
- Maximum enhancements in mass transfer coefficient of 35%, 245% and 207% were achieved in the presence of SiO_2, TiO_2 and ZrO_2, respectively.
- A new conceptual model was proposed for prediction of the effective diffusivity as a function of nanoparticle concentration, drop size and drop Reynolds number with a high accuracy.

GRAPHICAL ABSTRACT

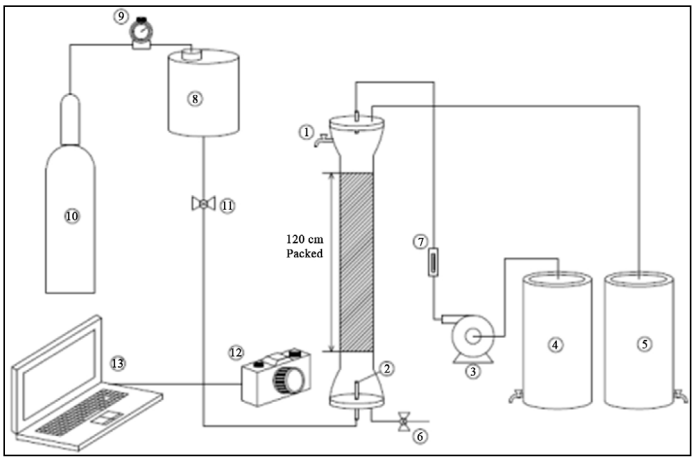

ARTICLE INFO

Article history:

Received 29 May 2017
Revised 9 Septmber 2017
Accepted 1 October 2017

Keywords:

Liquid-liquid extraction
Nanoparticles
Mass transfer coefficient
Hydrophobic
Hydrophilic

ABSTRACT

In the present study, the effect of various nanofluids on mass transfer coefficients in an irregular packed liquid-liquid extraction column was investigated. The chemical system of toluene-acetic acid-water was used. 10 nm SiO_2, TiO_2 and ZrO_2 nanoparticles with various concentrations were dispersed in toluene-acid acetic to provide nanofluids. The influence of concentration and hydrophobicity/hydrophilicity of nanoparticle on mass transfer coefficient was discussed. The experimental results show that the mass transfer coefficient enhancement depends on the kind and the concentration of nanoparticles. The Maximum enhancement of 35%, 245% and 207% was achieved for 0.05 vol% of SiO_2, TiO_2 and ZrO_2 nanofluids, respectively. A new conceptual model was proposed for prediction of the effective diffusivity as a function of nanoparticle concentration, drop size and drop Reynolds number.

* *Corresponding author: Tel.: +9821-77240496 ; Fax: +9821-77240397 ; E-mail address: ahmadrahbar@iust.ac.ir*

DOI: 10.22104/JPST.2017.2233.1084

1. Introduction

Nanofluids include various nanoparticles, such as metallic or nonmetallic, with a size less than 100 nm and have varied applications such as heat exchanger, medical, nuclear reactor, fuel cell, cooling of electronics, cameras, and displays [1].

Many researchers have worked on improving mass transfer with nanoparticles [2-11]. Recently, some researchers investigated the enhancement of mass transfer coefficients by nanoparticles in a liquid-liquid extraction process. Bahmanyar et al. evaluated mass transfer coefficients in a pulsed liquid-liquid extraction column using SiO_2 / kerosene nanofluids. They found that the mass transfer coefficient increased by 4-60% [12,13]. Saien et al. investigated mass transfer from nanofluids single drop in liquid-liquid extraction using two different nanofluids (γ-Al_2O_3/toluene and Fe_3O_4 / toluene) with and without a magnetic field [14,15]. They reported a maximum enhancement of 157% for the mass transfer rate. Rahbar et al. investigated the effect of type and concentration of nanoparticles on mass transfer coefficients [16]. Most researchers introduced the Brownian motion of the nanoparticles as the basic propellant for mass transfer enhancement.

In this work, the effect of various nanoparticles with different hydrophobic or hydrophilic properties and the same average size (10 nm) on the mass transfer coefficient in irregular packed liquid-liquid extraction columns has been investigated.

2. Experimental

2.1. Materials

Acetic acid (Merck, 99.9% w/w), toluene (Merck, 99% w/w) and deionized water were used. Deionized water and toluene with 0.05 vol% of acetic acid were used as the continuous phase and dispersed phase, respectively. Spherical SiO_2, TiO_2, and ZrO_2 nanoparticles with purities of more than 99.9% and the same average size (10 nm) were purchased from the TECNAN Company. The properties of the chemical materials and nanoparticles are given in Tables 1 and 2, respectively.

2.2. Experimental set-up

The experimental setup (Figure 1) consists of a Pyrex glass column (5.2 cm diameter and 1.6 m height) as the contactor. The stainless steel Raschig Ring random packings (0.9 porosity and 10 mm diameter) were used to fill the contactor. The column contains a perforated stainless steel tray to hold the packing. The packing height is 1.2 m in the column.

Three containers were used for the continuous phase, dispersed phase and the extract. The dispersed phase container was installed at a height of 2.5 meters from the ground level to supply sufficient pressure for the push dispersed phase into the continuous phase. The air pressure was applied on the dispersed phase. The dispersed phase enters the column bottom by a steel nozzle (17 cm length, 9.5 mm external diameter and 4.5 mm inner diameter). A solenoid valve was used to regulate the flow rate of the dispersed phase. The water enters through a peripheral pump at the top of the column. A rotameter was applied to have a constant water flow rate of 50 ml/min. Sampling was performed using the valve at the top of the column.

Table 1. Physical properties of chemical materials at 20 °C [17].

Property	Dispersed phase	Continuous phase
ρ (kg/m^3)	882.7	1009.7
μ (mPa.s)	0.611	1.016
γ (mN/m)	27.5 - 30.1	
D_d (m^2/s)	2.92×10^{-9}	

Table 2. Properties of nanoparticles.

Nanoparticle	Density (g/mL)	Specific surface (m^2/g)	Purity (%)
SiO_2	2.2	180-270	+99.9
TiO_2	3.84	100-150	+99.9
ZrO_2	5.68	70-105	+99.9

2.3. Preparation of nanofluids

The nanofluids were prepared by dispersing various concentrations of nanoparticles (0, 0.01, 0.05 and 0.1 vol%) into the dispersed phase. For this purpose a Hielscher ultrasonic vibrator was used for about one hour duration. The stability of nanofluids was evaluated by the sedimentation method.

2.4. Operation procedure

Before each experiment, both the continuous and

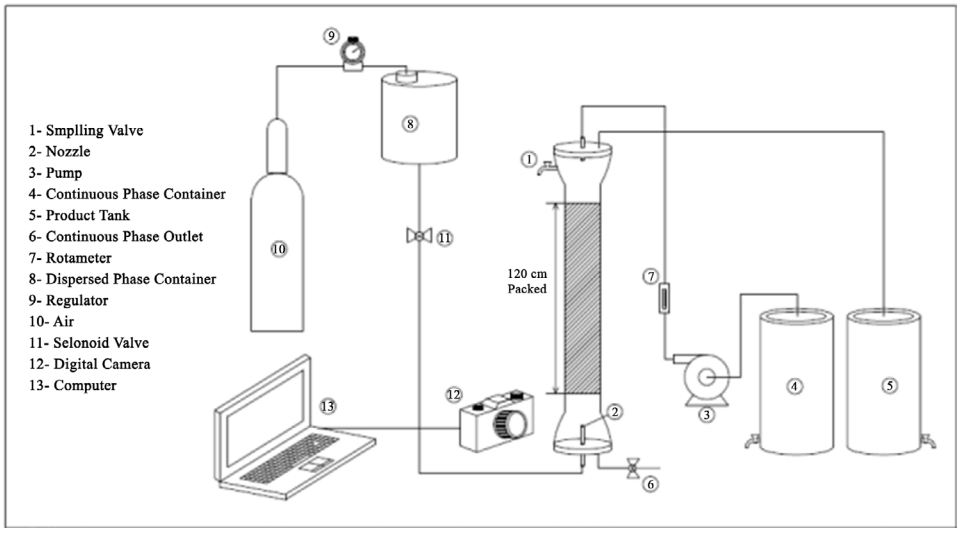

Fig. 1. Schematic diagram of the experimental setup.

the dispersed phases were saturated by each other. To beginning, the continuous phase entered from the top of the column, which was filled to the desired height. Afterward, the discharge valve of the continuous phase was opened such its level remains constant. The dispersed phase was then injected into the continuous phase from the bottom. The flow rate of the dispersed phase was set by the solenoid valve. If the pressure of the dispersed phase was not enough for dispersion into the continuous phase, the pressure was set by the pressure valve.

The diameter of the dispersed phase droplets was determined by taking digital photos. The mean diameter of the droplets was calculated by:

$$d = \frac{\sum n_i d_i^3}{\sum n_i d_i^2} \tag{1}$$

where n_i is the number of droplets and d_i is the measured droplet diameter.

In a steady state condition, sampling was carried out from the dispersed phase by the sampling valve and then was separated from the continuous phase by a decanter. The acetic acid concentration in the sample was determined by titration with a 0.1 N NaOH and in the presence of phenolphthalein indicator. 5 ml of sample was used for each titration.

Hold-up was determined by the shutdown method. At the end of each test run, the inlet and outlet valves of dispersed phase were closed simultaneously, and the droplets were allowed to coalesce at the interface. The hold-up was then calculated by:

$$\varphi = \frac{V_D}{V_D + V_C} \tag{2}$$

where, V_D and V_C are the collected volumes of the dispersed and continuous phases, respectively.

Mass transfer direction was from the dispersed phase to continuous phase. All experiments were performed at 25 °C.

2.5. Determination of the mass transfer coefficient

The mass transfer coefficient in the extractor is one of the most important parameters in industrial design. Considering the mass transfer during measured contact time, the mass balance relation is:

$$\dot{m}_1 - \dot{m}_2 = \frac{dm}{dt} \tag{3}$$

$$-N_{Ar}.S_r.M_A = \frac{d(n_A M_A)}{dt} = V_A \frac{dC_A}{dt} \tag{4}$$

$$-K_d(C_A - C_A^*).4\pi r^2 = \frac{4}{3}\pi r^3.\frac{dC_A}{dt} \tag{5}$$

The above mass balance is valid only if the droplet diameter and mass transfer coefficient remain constant while the drop rises through the column. By Integration of the equation, assuming the continuous phase to be completely mixed, the mass transfer coefficient can be obtained:

$$K_d = -\frac{d}{6t}\ln(1-E) \tag{6}$$

where

$$E = \frac{C_{A0} - C_A}{C_{A0} - C_A^*} \tag{7}$$

C_{A0} is the initial solute concentration, C_A is the final solute concentration in a specific position, and C_A^* is the equilibrium solute concentration. C_A was measured by titration and C_A^* can be assumed zero because the solute concentration in the continuous phase is negligible, d is the mean droplet diameter and t is the contact time which was obtained by [18]:

$$t = \frac{LS\varepsilon\varphi}{Q_d} \tag{8}$$

where L, S and ε are height, cross-sectional area, and voidage of the column, respectively. Q_d and φ are dispersed phase volume flow rate and hold-up.

3. Results and discussion

3.1. Stability of nanofuids

The nanofluids stability is shown in Figure 2. It was observed that the stability of SiO_2 was more than $TiO_2$and the stability of TiO_2 was also more than ZrO_2. It was concluded that the nanoparticles with lower density and hydrophobic property have better distribution stability.

3.2. Mass transfer coefficient

Experimental data for mass transfer coefficient s in the absence of nanoparticles are presented in Table 3. Tables 4, 5 and 6 provide all experimental data for mass transfer coefficients of SiO_2, TiO_2 and ZrO_2, respectively. It should be noted that each experiment was repeated two times and the average value of these two experiments was reported in the paper.

Figure 3 shows the effect of SiO_2 nanoparticles on the mass transfer coefficient. It was found that the mass transfer coefficient improves in the presence of SiO_2 nanoparticles and a maximum enhancement of 35% in a concentration of 0.05 vol% was achieved. This enhancement may be due to microconvection caused by Brownian motion of nanoparticles. It can be observed from Figure 3 that in higher concentrations of

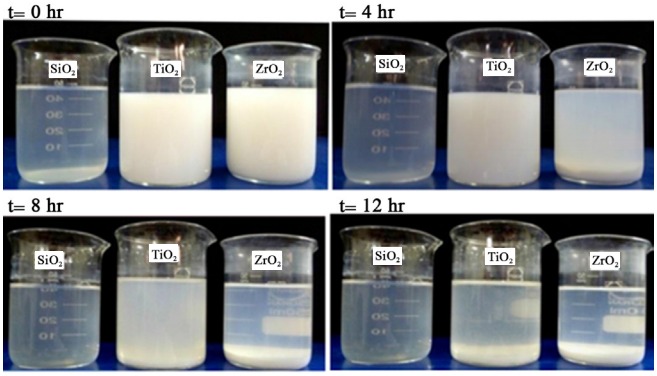

Fig. 2. Comparison of distribution stability for different nanoparticles in 0.1 vol%.

SiO_2 (usually more than 0.05 vol%) the mass transfer coefficient reduced due to aggregation of nanoparticles and a consequent reduction in the Brownian motion velocity.

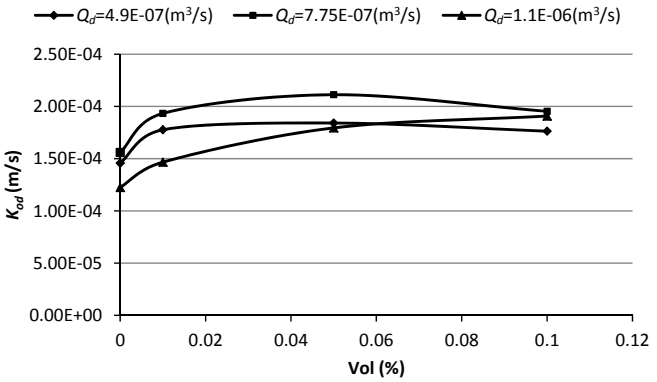

Fig. 3. Variation of mass transfer coefficient with concentration of SiO_2.

Figures 4-6 show mass transfer coefficient enhancement in the presence of TiO_2 and ZrO_2 nanoparticles. As observed, maximum enhancements of mass transfer coefficient were 245% and 207% for TiO_2 and ZrO_2 (in 0.05 vol%) , respectively, which was very significant. This high enhancement is not only caused by Brownian motion of nanoparticles. As shown in Figure 7, hydrophilic nanoparticles (TiO_2 and ZrO_2) tend to transfer from the organic phase to the aqueous phase which created turbulence at the interfacial surface, and consequently the mass transfer coefficient was significantly enhanced.

Table 3. Experimental data for mass transfer coefficients at the absence of nanoparticles.

Q_d (m^3/s)	d (mm)	Dynamic Hold up	E×100	t (s)	K_d×10^4 (m/s)	D_{eff} (m^2/s)
4.88×10^{-7}	9.11	0.006	93.56	28.6	1.46	9.96×10^{-8}
7.75×10^{-7}	8.71	0.008	92.41	24.0	1.56	1.03×10^{-7}
1.09×10^{-6}	8.30	0.012	89.66	25.6	1.23	7.73×10^{-8}

Table 4. Experimental data for mass transfer coefficients of SiO_2 particles.

Concentration (vol%)	Q_d (m^3/s)	d (mm)	Dynamic Hold-up	E×100	t (s)	K_d×10^4 (m/s)	D_{eff} (m^2/s)
0.01	4.88×10^{-7}	9.03	0.006	95.86	27.0	1.78	1.26×10^{-7}
	7.75×10^{-7}	9.63	0.008	93.10	22.2	1.93	1.32×10^{-7}
	1.09×10^{-6}	9.71	0.013	90.80	26.3	1.47	9.57×10^{-8}
0.05	4.88×10^{-7}	11.06	0.008	97.70	37.8	1.84	1.13×10^{-7}
	7.75×10^{-7}	11.75	0.009	94.48	26.9	2.11	1.91×10^{-7}
	1.09×10^{-6}	12.15	0.014	93.10	30.2	1.79	1.52×10^{-7}
0.10	4.88×10^{-7}	11.87	0.009	97.47	41.3	1.76	1.43×10^{-7}
	7.75×10^{-7}	12.65	0.010	93.79	30.0	1.95	1.49×10^{-7}
	1.09×10^{-6}	14.00	0.015	92.18	31.2	1.91	2.28×10^{-7}

Table 5. Experimental data for mass transfer coefficients of TiO_2 particles.

Concentration (vol%)	Q_d (m^3/s)	d (mm)	Dynamic Hold-up	E×100	t (s)	K_d×10^4 (m/s)	D_{eff} (m^2/s)
0.01	4.88×10^{-7}	9.2	0.003	98.85	14.1	4.86	3.75×10^{-7}
	7.75×10^{-7}	10.2	0.006	97.24	16.9	3.61	2.60×10^{-7}
	1.09×10^{-6}	10.7	0.009	96.78	18.1	3.39	2.44×10^{-7}
0.05	4.88×10^{-7}	10.5	0.004	99.20	16.8	5.03	3.38×10^{-7}
	7.75×10^{-7}	10.6	0.007	98.16	19.5	3.63	3.45×10^{-7}
	1.09×10^{-6}	11	0.011	97.70	22.6	3.06	2.78×10^{-7}
0.10	4.88×10^{-7}	10.6	0.004	99.35	18.1	4.91	4.42×10^{-7}
	7.75×10^{-7}	10.8	0.006	97.24	18.2	3.56	2.94×10^{-7}
	1.09×10^{-6}	12	0.010	96.09	21.1	3.08	3.90×10^{-7}

Table 6. Experimental data for mass transfer coefficients of ZrO_2 particles.

Concentration (vol%)	Q_d (m^3/s)	d (mm)	Dynamic Hold-up	E×100	t (s)	K_d×10^4 (m/s)	D_{eff} (m^2/s)
0.01	4.88×10^{-7}	9.5	0.003	97.70	14.1	4.24	3.25×10^{-7}
	7.75×10^{-7}	10.8	0.007	96.78	19.5	3.18	2.27×10^{-7}
	1.09×10^{-6}	11.5	0.009	96.09	18.7	3.33	2.39×10^{-7}
0.05	4.88×10^{-7}	10.1	0.004	98.85	16.8	4.48	2.99×10^{-7}
	7.75×10^{-7}	11.0	0.006	97.47	19.0	3.55	3.37×10^{-7}
	1.09×10^{-6}	12.2	0.009	96.55	19.6	3.50	3.21×10^{-7}
0.10	4.88×10^{-7}	10.2	0.004	98.53	16.8	4.26	3.80×10^{-7}
	7.75×10^{-7}	11.2	0.006	95.86	16.9	3.50	2.88×10^{-7}
	1.09×10^{-6}	12.5	0.008	94.25	17.2	3.47	4.44×10^{-7}

It can also be observed from Figures 4 and 5 that increasing the concentration of TiO_2 and ZrO_2 more than 0.05 vol% has no significant effect on the mass transfer coefficient. This is due to aggregation of nanoparticles. Aggregation of nanoparticles causes clusters of a hard solid media in the liquid phase. So it acts as an obstacle. As shown in Figure 6, mass transfer coefficient enhancement in the presence of TiO_2 and ZrO_2 was more significant than for SiO_2 because the mass transfer mechanism was affected by the transfer of hydrophilic nanoparticles (TiO_2 and ZrO_2) from the dispersed phase to the continuous phase, while SiO_2 was probably

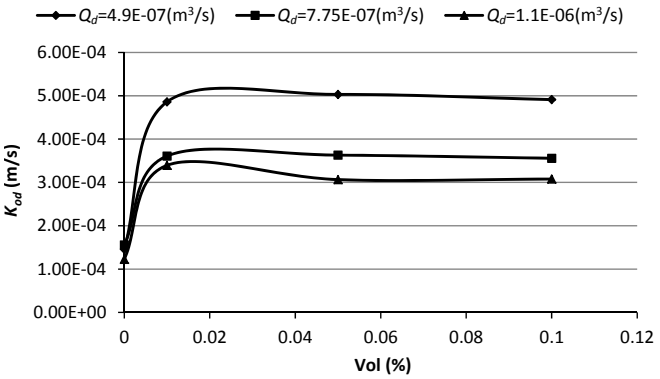

Fig. 4. Variation of mass transfer coefficient with concentration of TiO_2.

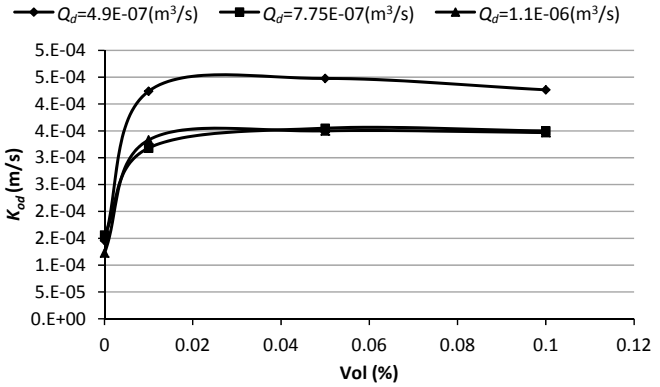

Fig. 5. Variation of mass transfer coefficient with concentration of ZrO_2.

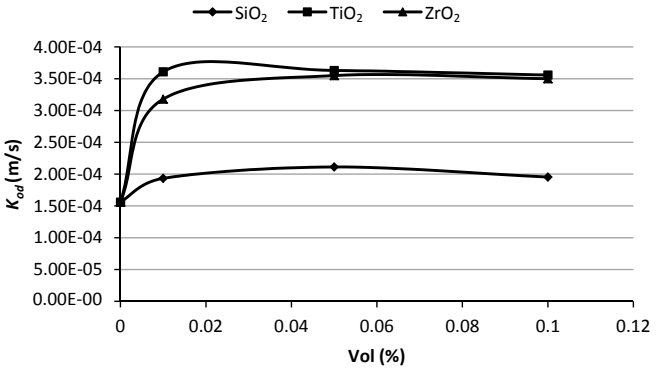

Fig. 6. Variation of mass transfer coefficient with concentration for various nanoparticles in Q_d = 7.75E-07 (m³/s).

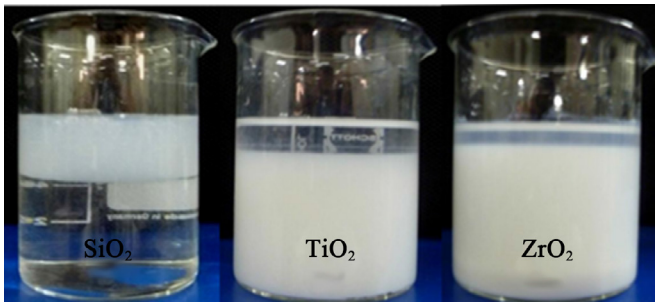

Fig. 7. Hydrophilic and hydrophobic properties of nanoparticles.

affected by the Brownian motion of the nanoparticles.

It can also be concluded from Figure 6 that the mass transfer coefficient in the presence of TiO_2 was more than ZrO_2. This is due to the super hydrophilicity and lower density of TiO_2 with respect to ZrO_2.

3.3. Predictive correlation for the effective diffusivity

The effective diffusivity was calculated from the experimental values of the mass transfer coefficients. To this purpose, molecular diffusivity (D_d) in the Newman equation (6) was replaced with effective diffusivity (D_{eff}) [19].

$$K_{od} = -\frac{d}{6t}\ln\left[\frac{6}{\pi^2}\sum_{n=1}^{\infty}\frac{1}{n^2}\exp\left(-\frac{4n^2\pi^2 D_d t}{d^2}\right)\right] \quad (9)$$

The calculated effective diffusivity for all drop size, nanoparticles concentrations (for n_c>0), and drop Reynolds number was fit to determine a predictive correlation. The predictive correlation is:

$$D_{eff} = a_1 \mathrm{Re}^{a_2}(d + a_3 n_c) - a_4 \quad (10)$$

The coefficients of the predictive model are reported in Table 7.

The average absolute relative error (*AARE*) for the effective diffusivity calculated with this predictive model compared with the experimental results is 9%. The % *AARE* is calculated by:

$$\%AARE = \frac{1}{N}\sum_{i=1}^{N}\left|\frac{Model - Experiment}{Experiment}\right| \times 100 \quad (11)$$

where, N is the number of data.

A comparison of the experimental effective diffusivities with those calculated by the proposed model is shown in Figure 8. This figure indicates that the suggested correlation can estimate the effective diffusivities with high accuracy. The predictive model shows that the effective diffusivity of hydrophilic nanoparticles (TiO_2 and ZrO_2) is also more dependant on nanoparticle concentration.

Table 7. The coefficients of the Predictive model.

Nanoparticle	a_1	a_2	a_3	a_4
SiO_2	1.27×10^{-6}	0.443	-2.65×10^{-3}	1.95×10^{-8}
TiO_2 & ZrO_2	2.75×10^{-6}	0.443	1.31×10^{-2}	3.35×10^{-8}

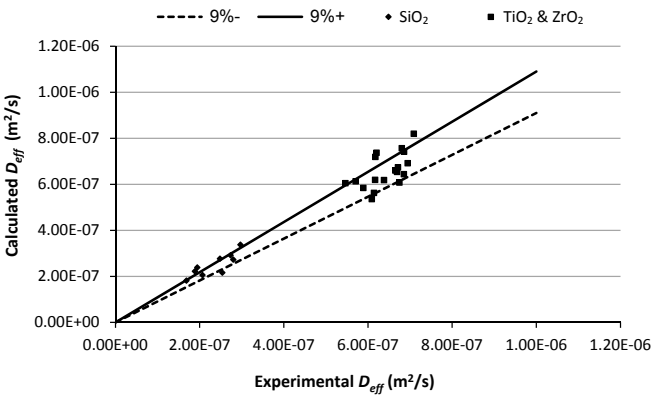

Fig. 8. Comparison of experimental and calculated D_{eff}.

4. Conclusion

In this study the effect of various nanoparticles with the same average size (10 nm) and different hydrophobic/hydrophilic property on the mass transfer coefficient was investigated. It was found through experimental data that the mass transfer coefficient was enhanced in the presence of nanoparticles. Maximum enhancements in the mass transfer coefficient of 35%, 245% and 207% were achieved in the presence of SiO_2, TiO_2 and ZrO_2, respectively, at a concentration of 0.05 vol%. A moderate enhancement in mass transfer coefficient (0-35%) may be due to Brownian motion of nanoparticles. But, the high enhancement in the mass transfer coefficient (more than 100%) in the presence of hydrophilic nanoparticles (TiO_2 and ZrO_2) was due to transfer of these nanoparticles from the organic to aqueous phase, which created a high turbulence on the interfacial surface. Unfortunately, the suspension of TiO_2 and ZrO_2 was too unstable and TiO_2 is too expensive. So, to achieve better mass transfer coefficient enhancement, the TiO_2 nanoparticle is suggested for this chemical system. The proposed model for prediction of effective diffusivity agreed well with the experimental data.

References

[1] R. Saidura, K.Y. Leongb, H.A. Mohammad, A review on applications and challenges of nanofluids, Renew. Sust. Energ. Rev. 15 (2011) 1646-1668.

[2] S. Krishnamurthy, P. Bhattacharya, P.E. Phelan, R.S. Prasher, Enhanced mass transport in nanofluids, Nano Lett. 6 (2006) 419-42.

[3] B. Olle, S. Bucak, T.C. Holmes, L. Bromberg, T.A. Hatton, D.I.C. Wang, Enhancement of oxygen mass transfer using functionalized magnetic nanoparticles, Ind. Eng. Chem. Res., 45 (2006) 4355-4363.

[4] H. Zhu, B.H. Shanks, T.J. Heindel, Enhancing CO-water mass transfer by functionalized MCM-41 nanoparticles, Ind. Eng. Chem. Res. 47 (2008) 7881-7887.

[5] X. Fang, Y. Xuan, Q. Li, Experimental investigation on enhanced mass transfer in nanofluids, Appl. Phys. Lett. 95 (2009) 203108.

[6] J. Veilleux, S. Coulombe, A total internal reflection fluorescence microscopy study of mass diffusion enhancement in water-based alumina nanofluids, Appl. Phys. 108 (2010) 104316-104318.

[7] J.K. Lee, J. Koo, H. Hong, Y.T. Kang, The effects of nanoparticles on absorption heat and mass transfer performance in NH_3/H_2O binary nanofluids, Int. J. Refrig. 33 (2010) 269-275.

[8] C. Pang, W. Wub, W. Sheng, H. Zhang, Y.T. Kang, Mass transfer enhancement by binary nanofluids (NH_3/H_2O + Ag nanoparticles) for bubble absorption process, In. J. Refrig. 35 (2012) 2240-2247.

[9] I.T. Pineda, J.W. Lee, I. Jung, Y.T. Kang, CO_2 absorption enhancement by methanol-based Al_2O_3 and SiO_2 nanofluids in a tray column absorber, Int. J. Refrig. 35 (2012) 1402-1409.

[10] H. Beiki, M. Nasr Esfahany, N. Etesami, Laminar forced convective mass transfer of g-Al_2O_3/electrolyte nanofluid in a circular tube, Int. J. Therm. Sci. 64 (2013) 251-256.

[11] H. Beiki, M. Nasr Esfahany, N. Etesami, Turbulent mass transfer of Al_2O_3 and TiO_2 electrolyte nanofluids in circular tube, Microfluid. Nanofluid. 15 (2013) 501-508.

[12] A. Bahmanyar, N. Khoobi, M.R. Mozdianfard, H. Bahmanyar, The influence of nanoparticles on hydrodynamic characteristics and mass transfer performance in a pulsed liquid-liquid extraction column, Chem. Eng. Process. 50 (2011) 1198-1206.

[13] A. Bahmanyar; N. Khoobi, M.M.A. Moharrer, H. Bahmanyar, Mass transfer from nanofluid drops in a pulsed liquid-liquid extraction column, Chem. Eng. Res. Des. 92 (2014) 2313-2323.

[14] J. Saien, H. Bamdadi, Mass transfer from nanofluid single drops inliquid-liquid extraction process, Ind. Eng. Chem. Res. 51 (2012) 5157-5166.

[15] J. Saien, H. Bamdadi, Sh. Daliri, Liquid-liquid extraction intensification with magnetite nanofluid single drops under oscillating magnetic field, Ind.

Eng. Chem. 21 (2014) 1152-1159.

[16] A. Rahbar-Kelishami, S.N. Ashrafizadeh, M. Rahnamaee, The effect of type and concentration of nano-particles on the mass transfer coefficients: experimental and Sherwood number correlating, Sep. Sci. Technol. 50 (2015) 1776-1784.

[17] A. Rahbar, Z. Azizi, H. Bahmanyar, M.A. Moosavian, Prediction of enhancement factor for mass transfer coefficient in regular packed liquid-liquid extraction columns, Can. J. Chem. Eng. 89 (2011) 508-519.

[18] R.E. Treybal, Mass transfer operations, 3rd Ed., McGraw Hill, Japan, 1990.

[19] A.B. Newman, The drying of porous solids: Diffusions and surface emission equations, T. Am. Inst. Chem. Eng. 27 (1931) 203-220.